Evolutionary divergence of protein structure: The linearly forced elastic network model

Article *in* Chemical Physics Letters · May 2008

DOI: 10.1016/j.cplett.2008.04.042

1 author:

Julian Echave
National University of General San Martín
113 PUBLICATIONS **1,880** CITATIONS

SEE PROFILE

Chemical Physics Letters 457 (2008) 413–416

Contents lists available at ScienceDirect

Chemical Physics Letters

journal homepage: www.elsevier.com/locate/cplett

Evolutionary divergence of protein structure: The linearly forced elastic network model

Julián Echave *

Universidad Nacional de La Plata, Instituto Nacional de Investigaciones Fisicoquímicas Teóricas y Aplicadas (INIFTA), CONICET-UNLP, Sucursal 4, Casilla de Correo 16, 1900 La Plata, Argentina

ARTICLE INFO

Article history:
Received 5 February 2008
In final form 10 April 2008
Available online 13 April 2008

ABSTRACT

The evolutionary divergence of protein structure is mostly contained within a subspace spanned by the evolving protein's lowest vibrational normal modes, a remarkable recent result, so far unexplained. To understand the mechanism underlying this behavior, here I introduce a linearly forced elastic network model (LFENM) of protein structural evolution. For a test case of globins, LFENM results are in very good agreement with observations. Moreover, in contrast with tentative biological explanations, the model predicts that protein structures will evolve along the lowest normal modes even under unselected random mutations, as a result of the chemical physics of the response of elastic networks of oscillators to perturbations.

1. Introduction

During protein evolution, their sequences, structures, dynamics, and function diverge due to mutation and natural selection. The importance of this process has resulted in much research on sequence evolution [1], structure evolution [2–5] and their interrelationship [1,6,7]. Recently, the evolution of protein dynamics has also been systematically studied [8]. Despite significant advances, developing a unified view of protein evolution is still an open problem [9].

The systematic study of protein structural divergence started about 20 yr ago with the seminal work of Chothia and Lesk, who found a correlation between divergence of sequences and structures and showed that structures diverge rather slowly, being more conserved than sequences [2]. Their results were later confirmed by others [3–5]. Recently, it was found that most of structural evolutionary divergence is contained within a subspace spanned by the lowest vibrational normal modes of the evolving proteins [10]. So far, we lack an explanation for these observations, except for the somewhat tentative interpretation that a presumed functional importance of the lowest normal modes could play a role [10,11]. To gain further insight into this issue the model of evolution of protein structure presented here was developed.

The model is based on elastic network models (ENM), which describe protein fluctuations using coupled harmonic oscillators [12–22]. ENMs reproduce very well the lowest normal modes [17,19–23] and have proved useful for a variety of problems [24–28]. For a recent review see [11]. Here, I add a linear perturbative term to the ENM Hamiltonian, to model the structural variations introduced by mutations. Natural selection is modeled using an acceptance probability function that depends on the mutation-induced structural perturbation. In what follows the model is called linearly forced elastic network model (LFENM). I will show that the LFENM is in very good agreement with experimental observations and it explains why protein structures diverge along the lowest normal modes.

2. Model of protein evolution

2.1. Elastic network model

At any step of the evolution of a given protein lineage, let the 'current protein' be called the 'wild type'. Let us consider the fluctuations of this protein around its equilibrium structure to be described by a coarse-grained elastic network model (ENM), which represents the protein as a network of nodes placed at the α carbons (C_α) connected by springs [11]. In general, the ENM potential is of the form

$$V_{\mathrm{wt}} = \frac{1}{2}(\mathbf{r} - \bar{\mathbf{r}}_{\mathrm{wt}})^T \mathbf{K} (\mathbf{r} - \bar{\mathbf{r}}_{\mathrm{wt}}) \tag{1}$$

where, for a protein of N sites, $\mathbf{r}$ is a column vector with $3N$ elements: the x, y, z coordinates of the N C_α, $\bar{\mathbf{r}}$ is the equilibrium structure, and $\mathbf{K}$ is the 'stiffness' matrix, which represents the network topology and spring force constants.

2.2. Linearly forced elastic network model

The first elementary step of protein evolution is the introduction of random mutations, due to errors in gene replication. Here

* Fax: +54 221 4257291.
E-mail address: jechave@inifta.unlp.edu.ar

0009-2614/$ - see front matter © 2008 Elsevier B.V. All rights reserved.
doi:10.1016/j.cplett.2008.04.042

I will consider only point mutations (amino acid replacements), which are the most frequent. Mutants are modeled by adding a linearly forcing term to Eq. (1):

$$V_{\mathrm{mut}} = V_{\mathrm{wt}} - \mathbf{f}^T(\mathbf{r} - \bar{\mathbf{r}}_{\mathrm{wt}}) \tag{2}$$

where $\mathbf{f}$ is a column vector with $3N$ elements that models the mutation. Note that $\mathbf{f} = -(\frac{\partial V_{\mathrm{mut}}}{\partial \mathbf{r}})_{\mathbf{r}=\bar{\mathbf{r}}_{\mathrm{wt}}}$ is the force that moves the mutant structure away from the wild-type structure.

The equilibrium structure of the mutant $\bar{\mathbf{r}}_{\mathrm{mut}}$ is the value of $\mathbf{r}$ which minimizes V_{mut}. Using Eqs. (1) and (2) we find the structural variation due to the mutation:

$$\delta\bar{\mathbf{r}} \equiv \bar{\mathbf{r}}_{\mathrm{mut}} - \bar{\mathbf{r}}_{wt} = \mathbf{K}^{-1}\mathbf{f} \tag{3}$$

This equation shows that the structural perturbation introduced by mutation is related to the mutation ($\mathbf{f}$) and to the network of oscillators, via $\mathbf{K}^{-1}$. The latter is responsible of the larger contribution of the lowest normal modes to evolutionary deformations, as shown below.

To complete the model of evolution, we need to consider natural selection. I model selection by assigning to each mutant an acceptance probability:

$$p(\delta\bar{\mathbf{r}};\beta) = \exp(-\beta\delta\bar{\mathbf{r}}^T\mathbf{K}\delta\bar{\mathbf{r}}) \tag{4}$$

where $\beta \geqslant 0$ is a parameter that allows tuning the selection pressure against structural variation. Note that $\beta = 0$ corresponds to the purely mutational model, whereas for $\beta > 0$ the acceptance probability decreases with increasing $\|\delta\bar{\mathbf{r}}\|$. Since mutants have lower fitness than the (current) wild type, this is sometimes called 'negative selection' or 'purifying selection'. I will show elsewhere that this selection function can be derived from the neutral theory of evolution [29] by assuming that the so called 'selective advantage' (the fitness difference between the mutant and the wild-type) is given by $s = -\beta\delta\bar{\mathbf{r}}^T\mathbf{K}\delta\bar{\mathbf{r}}$. In this sense, this is a 'neutral evolution' model. From a different perspective, we note that since Eq. (4) is proportional to the Boltzmann probability that the mutant will adopt the wild-type conformation, $p(\delta\bar{\mathbf{r}};\beta)$ can be interpreted as the mutant's degree of activity.

To summarize, the linearly forced elastic network model (LFENM) of protein structural divergence is specified by Eqs. (2) and (3), which model the mutation, and by Eq. (4), which models natural selection.

2.3. Model parameters and numerical details

To completely specify the model, we must choose $\mathbf{K}$ and $\mathbf{f}$. There are a number of alternative ENMs and thus $\mathbf{K}$ (see e.g. [14,15,17,20]). Here I have used the 'beta Gaussian Network Model' (βGNM), which builds $\mathbf{K}$ from the coordinates of C_α and C_β, and uses a higher force constant for covalently bonded residues than for non-bonded ones. For a detailed description see [17].

To calculate $\mathbf{f}$, given a mutation at a site l, each site i in contact with l is assigned a force $\mathbf{f}_{l\to i}$ directed along the l–i contact and site l is assigned a reaction force $\mathbf{f}_l = -\sum_{i\neq l}\mathbf{f}_{l\to i}$. To simulate random mutations, the magnitudes of $\mathbf{f}_{l\to i}$ were randomly picked from a uniform distribution in $[-f_{\max}, f_{\max}]$. The forces for different contacts were picked independently. Since $f_{\max}$ does not affect the results, we set $f_{\max} = 1$.

This way of describing mutations lacks chemical specificity. However, this is consistent with the lack of chemical specificity of ENM models, which in general do not depend on amino acid sequence. Moreover, during evolution, despite conservation of function and structure, protein sequences diverge significantly. Finally, we can think of the range of the parameter $[-f_{\max}, f_{\max}]$ as a continuous approximation of the perturbations introduced by the $20 \times 19 = 380$ possible mutations, covering from mutations between physicochemically similar amino acids ($f \sim 0$) up to mutations between very different amino acids ($f \sim \pm f_{\max}$).

The dataset of mutants analyzed corresponds to mutants that differ in 1 site from the protein (wild type) studied. A large dataset was built by generating 100 mutants for each site of wild type. It should be noted that no lineages are simulated here but, rather, the immediate 1-mutation neighborhood of the wild type is considered. For each mutant I calculated $\delta\bar{\mathbf{r}}$ – Eq. (3) and $p(\delta\bar{\mathbf{r}};\beta)$ – Eq. (4). To study the effect of selection pressure, I used $\beta \in \{0, 1, 5, 10, 25, 50, 75, 100\}$. In this way, a set of N_{mut} mutants with their structures and selection probabilities were obtained and used for the analysis described next.

2.4. Analysis

First, I calculated the acceptance rate which measures the proportion of accepted mutants:

$$\omega \equiv \frac{\sum p(\delta\bar{\mathbf{r}};\beta)}{N_{\mathrm{mut}}} \tag{5}$$

where the sum is over the N_{mut} mutants. The overall structural variation was calculated using:

$$\langle\|\delta\bar{\mathbf{r}}\|^2\rangle \equiv \frac{\sum p(\delta\bar{\mathbf{r}};\beta)\|\delta\bar{\mathbf{r}}\|^2}{\sum p(\delta\bar{\mathbf{r}};\beta)} \tag{6}$$

The root mean square deviation is $\mathrm{RMSd} \equiv \sqrt{\langle\|\delta\bar{\mathbf{r}}\|^2\rangle}$.
Second, the normal modes $\mathbf{q}_n$ and eigenvalues λ_n were obtained from:

$$\mathbf{K}\mathbf{q}_n = \lambda_n\mathbf{q}_n \tag{7}$$

There are $3N$-6 non-zero eigenvalues, which correspond to the vibrational modes, numbered $n = 0, 2, \ldots, 3N-7$.

Third, I calculated the average relative contribution of each normal mode to the total structural variation using:

$$P_n \equiv \frac{\langle(\mathbf{q}_n^T\delta\bar{\mathbf{r}})^2\rangle}{\langle\|\delta\bar{\mathbf{r}}\|^2\rangle} \tag{8}$$

where the average is over all mutants weighted by the selection probabilities as in Eq. (6). The cumulative contribution of modes *0-n* was also obtained:

$$Q_n \equiv \sum_{m=0}^{n} P_m \tag{9}$$

Finally, to compare with experimental data, P_n and Q_n were also calculated for the variation of the conserved structural core (see Section 3), using Eqs. (8) and (9) with $\delta\bar{\mathbf{r}}_{\mathrm{core}}$ in place of $\delta\bar{\mathbf{r}}$. For each mutant $\delta\bar{\mathbf{r}}_{\mathrm{core}}$ was obtained by projecting $\delta\bar{\mathbf{r}}$ onto the core.

3. Test case: globins

The test case used is the sperm-whale myoglobin with Protein Data Base (PDB) code 1a6m as the 'wild-type'. This protein is a 151 long monomer. The heme was considered in the ENM by using five extra nodes to model Fe and the four porphyrin rings. Starting from 1a6m, I calculated $100 \times 151 = 15\,100$ single point mutants, their structures, and probabilities, as described in Section 2.3.

The experimental structural divergence was obtained by analyzing 1a6m and 22 homologous globins used by Leo-Macias et al. [10]: 1dlwa, 1dlya, 1dra, 1kr7a, 1sdha, 1b0b, 1h97a, 1jl7a, 1mba, 1eco, 2gdm, 1irda, igcva, 1fhjb, 1cg5b, 1gcvb, 1it2a, iash, i1tha, 1hlb, 1cqxa, 1ew6a. The first four characters are the PDB code and for multimeric proteins the fifth one is the chain ID. These proteins were structurally aligned using MAMMOTH [30]. A conserved structural core of 75 sites is obtained, which consists of aligned positions with no gaps and with low structural divergence

[30]. Then, for each protein p, a vector of core C_α coordinates $\bar{\mathbf{r}}^p_{\text{core}}$ was obtained, and all structural differences $\Delta\bar{\mathbf{r}}^{pq}_{\text{core}} = \bar{\mathbf{r}}^p - \bar{\mathbf{r}}^q$ were calculated. These were projected onto the normal modes of 1a6m to calculate the contributions P_n and Q_n using Eqs. (8) and (9) with $\Delta\bar{\mathbf{r}}^{pq}_{\text{core}}$ in place of $\delta\bar{\mathbf{r}}$.

4. Results and discussion

Fig. 1 shows the acceptance rate ω – Eq. (5) and the average structural perturbation $\langle\|\delta\bar{\mathbf{r}}\|^2\rangle$ – Eq. (6) as a function of selection pressure β. For $\beta = 0$ all mutations are accepted: $\omega = 1$. As β increases ω decreases. Similarly, $\langle\|\delta\bar{\mathbf{r}}\|^2\rangle$ decreases with increasing β. For higher β, mutants with larger $\|\delta\bar{\mathbf{r}}\|$ will be discarded by natural selection – Eq. (4) – making both the proportion of accepted mutants and the average structural perturbation decrease.

Fig. 2 shows the normal mode contributions to LFENM structural divergence P_n and Q_n for two cases: $\beta = 0$ – unselected mutations – and $\beta = 10$, for which more than 50% of mutants are discarded. Clearly, despite the effect of selection on decreasing the total structural variation $\langle\|\delta\bar{\mathbf{r}}\|^2\rangle$ (see Fig. 1) there is almost no effect on the profile of relative normal mode contributions: P_n and Q_n for both β values overlap almost perfectly. This is also the case for the other β values considered (data not shown): selection does not affect the P_n and Q_n profiles that result just from random mutations.

Fig. 2 also shows that P_n decreases with increasing n. Thus, the LFENM predicts that even under no selection, the lowest normal modes will contribute the most to evolutionary deformations. Therefore, from the Q_n plots we see that a few of the lowest modes are needed to account for most of the structural variation. For example, ~9% of the modes account for 64% of $\langle\|\delta\bar{\mathbf{r}}\|^2\rangle$ (i.e. 80% of the RMSd). Thus, most structural divergence occurs within a subspace spanned by the lowest normal modes even under unselected random mutations.

Fig. 3 shows that $P_n \propto 1/\lambda_n$ for LFENM with $\beta = 0$ (and also for the other β values, not shown): normal modes contribute to structural divergence proportionally to their inverse eigenvalues. The fit is very good, with a correlation coefficient $r = 0.98$.

Since the site-site correlation matrix for the unperturbed elastic network is $\mathbf{K}^{-1}$ [13,14], it can easily be shown that the average square fluctuations due to the protein dynamics scales as $\langle(\mathbf{q}_n^T\delta\mathbf{r})^2\rangle_{\text{dyn}} \propto 1/\lambda_n$. This, together with the fluctuation–dissipation theorem, which states that the linear response of a given system to an external perturbation is expressed in terms of fluctuation properties of the system in thermal equilibrium, may mislead us to think that the results of Fig. 3 are a trivial consequence of the scaling behavior of dynamical deformations. A more careful analysis shows that replacing Eq. (3) into Eq. (8) and using Eq. (7), we find:

$$P_n \propto \lambda_n^{-2}\langle f_n^2\rangle \tag{10}$$

where $f_n \equiv \mathbf{q}_n^T\mathbf{f}$ is the projection of $\mathbf{f}$ onto mode n, and the average is taken over all mutants. Therefore, it is not *a priori* obvious that $P_n \propto 1/\lambda_n$. Rather, from the simulated data it is found that $\langle f_n^2\rangle \propto \lambda_n$ (not shown), so that there is a partial compensation in Eq. (10), which results in $P_n \propto \lambda_n^{-1}$. The fact that $\langle f_n^2\rangle \propto \lambda_n$ is not true of any force, but can be demonstrated analytically for the force used here to model mutations. The key issue is that since the force used is directed along contacts, it has the same structure as the stiffness matrix. Such demonstration is beyond the scope of this letter and will be presented elsewhere.

Finally, Fig. 4 shows the LFENM-experimental comparison of the profiles of normal mode contributions to the structural divergence of the conserved core. Only the conserved core can be considered because with current structural alignment methods the most structurally divergent regions cannot be aligned. Fig. 4 shows that there is very good agreement between LFENM and observed data both in P_n and Q_n. To quantify this accord, we calculated the

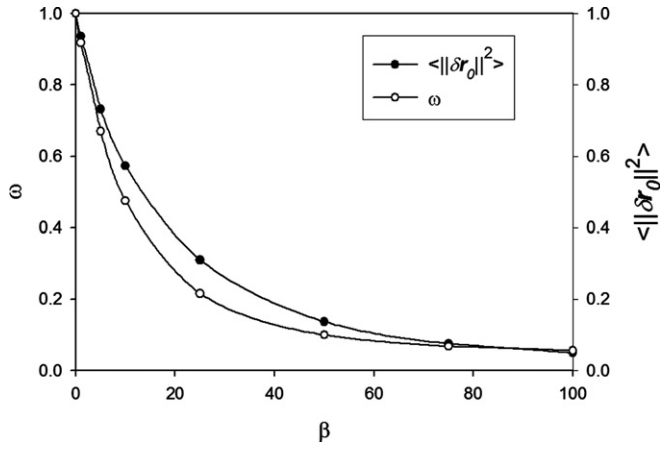

Fig. 1. Effect of selection pressure on acceptance rate and total structural variation. β is the LFENM selection parameter of Eq. (4); ω (empty circles) and $\langle\|\delta\bar{\mathbf{r}}\|^2\rangle$ (filled circles) were calculated using Eqs. (5) and (6), respectively. The latter was divided by its value at $\beta = 0$.

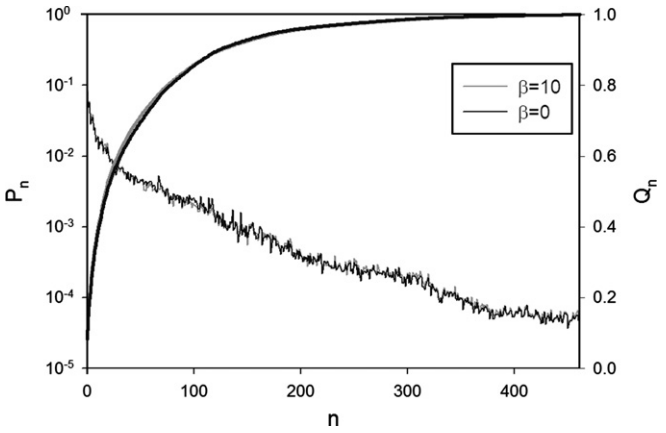

Fig. 2. LFENM structural divergence along normal modes. P_n for unselected mutations: $\beta = 0$ (fine black line) and moderate selection: $\beta = 10$ (fine grey line) are shown. Cumulative contributions Q_n are also shown for $\beta = 0$ (broad black line) and $\beta = 10$ (broad grey line). P_n and Q_n were calculated using Eq. (8) and Eq. (9), respectively.

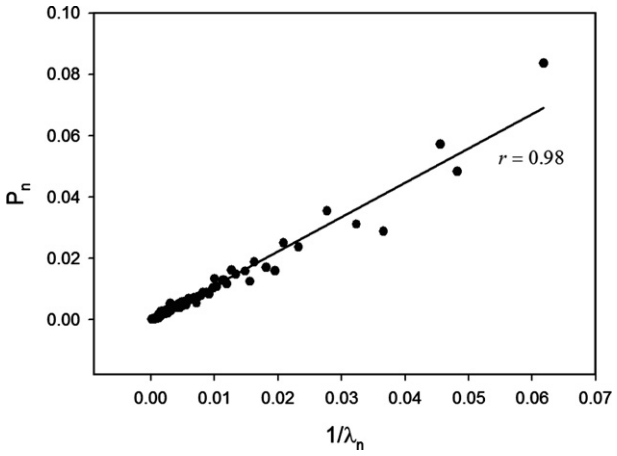

Fig. 3. LFENM structural divergence along normal modes vs. $1/\lambda_n$. For normal mode n, λ_n is the eigenvalue and P_n is calculated using Eq. (8). Results shown correspond to LFENM simulations with $\beta = 0$.

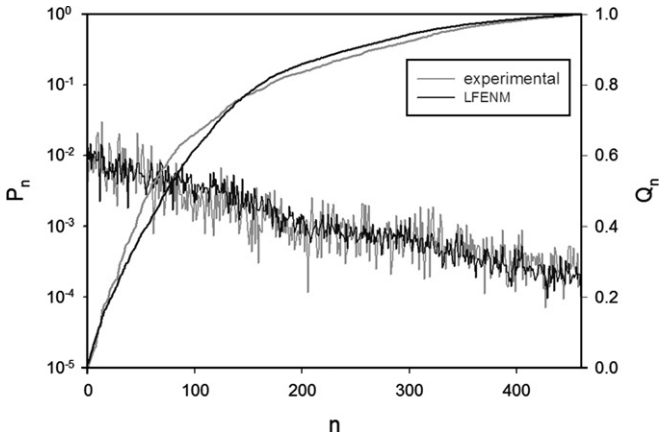

Fig. 4. LFENM vs. experimental structural divergence of the conserved core along normal modes. P_n for $\beta = 0$ LFENM simulations (fine black lines) are compared with the experimental ones (fine gray line). Cumulative contributions Q_n are also shown: LFENM (broad black lines) and experimental (broad gray lines). P_n and Q_n were calculated using Eq. (8) and Eq. (9), respectively.

Pearson correlation coefficient between experimental vs. LFENM data and found $r = 0.81$, which is highly significant. The experimental data are somewhat noisier, due to the rather low number of proteins considered. In both cases the general tendency is a decrease of P_n with increasing n. From the Q_n plots, we see that 23% of the normal modes are needed to account for 64% $\langle \|\delta\vec{\mathbf{r}}_{\text{core}}\|^2 \rangle$ (80% of RMSd).

It is worthwhile to compare the total structural divergence (Fig. 2) with the conserved core divergence (Fig. 4). The former shows a much stronger decrease of P_n with n and a corresponding sharper increase of Q_n. Thus, to cover 80% of the total RMSd, 9% of the modes are enough, whereas 23% are necessary to cover 80% of the core RMSd. This results from projecting the total structural variation onto the conserved core. Such projection results in a large underestimation of the contribution of the lowest normal modes to the total structural divergence. In spite of this, even for the core the tendency of increasing contributions for lowest normal modes is clear, in agreement with what was reported in [10].

5. Conclusion

I presented the linearly forced elastic network model of protein structural evolution. The model accounts for the recent observation that evolutionary deformations lie within a subspace spanned by the lowest vibrational normal modes. Moreover, it provides a mechanism that explains this behavior. Even unselected random mutations would result in structural drift along the directions of the lowest normal modes. This results simply from the chemical physics of the response of the protein to random mutations: a local perturbation is propagated through the elastic network, via Eq. (3), producing a collective structural change within the spaced spanned by the lowest normal modes.

It is worthwhile to consider briefly the parallels between evolutionary deformations and conformational changes induced by ligand binding. Ligand-induced conformational changes are also contained within a subspace spanned by the lowest ENM normal modes [28,31–34]. Clearly the LFENM – Eq. (2) – could also model ligand-induced conformational transitions, with a force appropriately adapted to model ligand binding. Thus, the LFENM could also explain the larger contribution of the lowest normal modes to conformational transitions. In a related approach, a Linear Response Approximation has been used to predict ligand-induced conformational changes [35].

I should mention, before ending, possible caveats of the present results. First, the model of mutation does not depend on the chemical nature of the mutated amino acids. As explained in Section 2.3, this is a reasonable first approximation. More importantly, the model does agree with experiment. In addition to validating the model, this means that the observed statistical behavior of evolutionary deformations is to be expected from the response of a network of oscillators to random perturbations, without requiring a detailed account of the chemical details of mutations. Second, the model uses a neutral evolution selection function, which could be considered a weakness. However, apart from being consistent with the data supporting the neutral theory, the model-experiment agreement was found to be independent of selection: it is mutation, not selection, the reason behind the larger contribution of the lowest normal modes to evolutionary deformations. Thus, we expect the present results to hold even under positive selection.

Apart from the issues considered here, this model should be useful for applied purposes such as protein structure alignment, homology modeling, and structure-based phylogenetic inference, among others.

Acknowledgements

I thank Cristian Micheletti for sending me his βGNM code, Alejandra Leo-Macias and Angel Ortiz for their data on structural divergence, and Ugo Bastolla and Angel Ortiz for fruitful discussions. This work was supported by CONICET and ANPCyT.

References

[1] J.L. Thorne, Curr. Opin. Genet. Dev. 10 (2000) 602.
[2] C. Chothia, A.M. Lesk, Embo J. 5 (1986) 823.
[3] B. Rost, Fold. Des. 2 (1997) S19.
[4] T.C. Wood, W.R. Pearson, J. Mol. Biol. 291 (1999) 977.
[5] P. Koehl, M. Levitt, J. Mol. Biol. 323 (2002) 551.
[6] G. Parisi, J. Echave, Mol. Biol. Evol. 18 (2001) 750.
[7] M. Porto, H.E. Roman, M. Vendruscolo, U. Bastolla, Mol. Biol. Evol. 22 (2005) 630.
[8] S. Maguid, S. Fernandez-Alberti, G. Parisi, J. Echave, J. Mol. Evol. 63 (2006) 448.
[9] C. Pal, B. Papp, M.J. Lercher, Nat. Rev. Genet. 7 (2006) 337.
[10] A. Leo-Macias, P. Lopez-Romero, D. Lupyan, D. Zerbino, A.R. Ortiz, Biophys. J. 88 (2005) 1291.
[11] I. Bahar, A.J. Rader, Curr. Opin. Struct. Biol. 15 (2005) 586.
[12] M.M. Tirion, Phys. Rev. Lett. 77 (1996) 1905.
[13] I. Bahar, A.R. Atilgan, B. Erman, Fold. Des. 2 (1997) 173.
[14] T. Haliloglu, I. Bahar, B. Erman, Phys. Rev. Lett. 79 (1997) 3090.
[15] A.R. Atilgan, S.R. Durell, R.L. Jernigan, M.C. Demirel, O. Keskin, I. Bahar, Biophys. J. 80 (2001) 505.
[16] M. Delarue, Y.H. Sanejouand, J. Mol. Biol. 320 (2002) 1011.
[17] C. Micheletti, P. Carloni, A. Maritan, Proteins 55 (2004) 635.
[18] Y.H. Jang, J.I. Jeong, M.K. Kim, Nucleic Acids Res. 34 (2006) W57.
[19] D.M. Ming, R. Bruschweiler, Biophys. J. 90 (2006) 3382.
[20] G. Song, R.L. Jernigan, J. Mol. Biol. 369 (2007) 880.
[21] L.W. Yang, E. Eyal, C. Chennubhotla, J. Jee, A.M. Gronenborn, I. Bahar, Structure 15 (2007) 741.
[22] T. Mamonova, A. Ramanathan, M. Kurnikova, Biophys. J. (2007) 376A.
[23] M. Rueda, P. Chacon, M. Orozco, Structure 15 (2007) 565.
[24] K. Hinsen, Proteins 33 (1998) 417.
[25] J.B. He, Z.Y. Zhang, Y.Y. Shi, H.Y. Liu, J. Chem. Phys. 119 (2003) 4005.
[26] L.W. Yang, X. Liu, C.J. Jursa, M. Holliman, A. Rader, H.A. Karimi, I. Bahar, Bioinformatics 21 (2005) 2978.
[27] D.A. Kondrashov, Q.A. Cui, G.N. Phillips, Biophys. J. 91 (2006) 2760.
[28] W.J. Zheng, B.R. Brooks, D. Thirumalai, Proc. Natl. Acad. Sci. USA 103 (2006) 7664.
[29] M. Kimura, The Neutral Theory of Molecular Evolution , Cambridge University Press, Cambridge, UK, 1983.
[30] A.R. Ortiz, C.E.M. Strauss, O. Olmea, Protein Sci. 11 (2002) 2606.
[31] D. Tobi, I. Bahar, Proc. Natl. Acad. Sci. USA 102 (2005) 18908.
[32] E. Lindahl, M. Delarue, Nucleic Acids Res. 33 (2005) 4496.
[33] B. Erman, Biophys. J. 91 (2006) 3589.
[34] O. Keskin, Bmc Struct. Biol. 7 (2007) 31.
[35] M. Ikeguchi, J. Ueno, M. Sato, A. Kidera, Phys. Rev. Lett. 94 (2005) 078102.